Clinical Cancer Research

Nintedanib Is Active in Malignant Pleural Mesothelioma Cell Models and Inhibits Angiogenesis and Tumor Growth *In Vivo*

Viktoria Laszlo[1,2], Zsuzsanna Valko[1,3], Ildiko Kovacs[3], Judit Ozsvar[1], Mir Alireza Hoda[1], Thomas Klikovits[1], Dora Lakatos[4], Andras Czirok[4,5], Tamas Garay[6,7], Alexander Stiglbauer[2], Thomas H. Helbich[2], Marion Gröger[8], Jozsef Tovari[9,10], Walter Klepetko[1], Christine Pirker[11], Michael Grusch[11], Walter Berger[11], Frank Hilberg[12], Balazs Hegedus[1,6,7,13], and Balazs Dome[1,2,3,14]

Abstract

Purpose: Malignant pleural mesothelioma (MPM) is an aggressive thoracic tumor type with limited treatment options and poor prognosis. The angiokinase inhibitor nintedanib has shown promising activity in the LUME-Meso phase II MPM trial and thus is currently being evaluated in the confirmatory LUME-Meso phase III trial. However, the anti-MPM potential of nintedanib has not been studied in the preclinical setting.

Experimental Design: We have examined the antineoplastic activity of nintedanib in various *in vitro* and *in vivo* models of human MPM.

Results: Nintedanib's target receptors were (co)expressed in all the 20 investigated human MPM cell lines. Nintedanib inhibited MPM cell growth in both short- and long-term viability assays. Reduced MPM cell proliferation and migration and the inhibition of Erk1/2 phosphorylation were also observed upon nintedanib treatment *in vitro*. Additive effects on cell viability were detected when nintedanib was combined with cisplatin, a drug routinely used for systemic MPM therapy. In an orthotopic mouse model of human MPM, survival of animals receiving nintedanib *per os* showed a favorable trend, but no significant benefit. Nintedanib significantly reduced tumor burden and vascularization and prolonged the survival of mice when it was administered intraperitoneally. Importantly, unlike bevacizumab, nintedanib demonstrated significant *in vivo* antivascular and antitumor potential independently of baseline VEGF-A levels.

Conclusions: Nintedanib exerts significant antitumor activity in MPM both *in vitro* and *in vivo*. These data provide preclinical support for the concept of LUME-Meso trials evaluating nintedanib in patients with unresectable MPM. *Clin Cancer Res; 24(15); 3729–40. ©2018 AACR.*

Introduction

Malignant pleural mesothelioma (MPM) is a rare but aggressive thoracic malignancy that originates from the pleural mesothelium. MPM is most often caused by asbestos but causal links to ionizing radiation have also been suggested (1). Notably, germline mutations in a tumor suppressor gene, *BAP1 (BRCA1 associated protein-1*), were shown in families with high MPM incidence (2).

There are three main histological subtypes of MPM: epithelioid, sarcomatoid, and biphasic. The latter two subtypes are especially refractory to therapy and thus patients with sarcomatoid or biphasic MPM have poorer outcomes than those with epithelioid tumors (3). Although local invasion and recurrence are pathognomonic features of MPM, a study on a large postmortem series demonstrated that extrathoracic metastases are common (4).

Because MPM presents with advanced stage in most cases, many MPM patients receive systemic therapy either alone or as part of multimodality treatment. The combination of cisplatin with pemetrexed is the standard first-line systemic therapy (5). The recently published phase III MAPS study, however, demonstrated that the addition of bevacizumab, a VEGF (vascular endothelial growth factor) neutralizing antibody, to this combination significantly prolongs patients' overall survival (OS) (6). Accordingly, the latest NCCN guideline recommends bevacizumab/cisplatin/pemetrexed as a first-line

[1]Division of Thoracic Surgery, Department of Surgery, Comprehensive Cancer Centre Vienna, Medical University Vienna, Austria. [2]Department of Biomedical Imaging and Image-guided Therapy, Division of Molecular and Gender Imaging, Medical University of Vienna, Vienna, Austria. [3]National Koranyi Institute of Pulmonology, Budapest, Hungary. [4]Department of Biological Physics, Eotvos University, Budapest, Hungary. [5]Department of Anatomy and Cell Biology, University of Kansas Medical Center, Kansas City, Kansas. [6]2nd Department of Pathology, Semmelweis University, Budapest, Hungary. [7]Tumor Progression Research Group, Hungarian Academy of Sciences-Semmelweis University, Budapest, Hungary. [8]Core Facility Imaging, Core Facilities, Medical University Vienna, Austria. [9]Department of Experimental Pharmacology, National Institute of Oncology, Budapest, Hungary. [10]Kineto Lab Ltd., Budapest, Hungary. [11]Institute of Cancer Research and Comprehensive Cancer Center, Department of Medicine I, Medical University of Vienna, Austria. [12]Boehringer Ingelheim RCV GmbH, Vienna, Austria. [13]Department of Thoracic Surgery, Ruhrlandklinik, University Duisburg-Essen, Germany. [14]Department of Thoracic Surgery, National Institute of Oncology-Semmelweis University, Budapest, Hungary.

Note: Supplementary data for this article are available at Clinical Cancer Research Online (http://clincancerres.aacrjournals.org/).

B. Dome and B. Hegedus contributed equally as senior authors to this article.

Corresponding Authors: Balazs Dome, Medical University Vienna, Waehringer Guertel 18-20, Vienna, Austria 1090. Phone: 43-1-40400-56440; Fax: 43-1-40400-5642; E-mail: balazs.dome@meduniwien.ac.at; and Balazs Hegedus, Department of Thoracic Surgery, Ruhrlandklinik, University Clinic Essen, University Duisburg-Essen; Tüschener Weg 40, 45239 Essen, Germany. Phone: 492014334665; E-mail: Balazs.Hegedues@rlk.uk-essen.de

doi: 10.1158/1078-0432.CCR-17-1507

Translational Relevance

Malignant pleural mesothelioma (MPM) is an aggressive thoracic malignancy with dismal prognosis. Accordingly, there has been increased interest in targeted drugs against this tumor type. The triple angiokinase inhibitor nintedanib is approved for the treatment of idiopathic pulmonary fibrosis and of lung adenocarcinoma. Here, we demonstrate that human MPM cells express the target receptors of nintedanib and, furthermore, that nintedanib inhibits the growth, proliferation, and migration of MPM cells *in vitro*. Moreover, we show that in mice with orthotopically growing human MPM xenografts, nintedanib potently reduces tumor growth and vascularization. Importantly, this *in vivo* antivascular and antitumor effect of nintedanib is more potent than that of bevacizumab in the treatment of tumors with low baseline VEGF-A expression. In conclusion, our preclinical findings—together with the positive LUME-Meso clinical trial data—indicate that nintedanib is a promising agent for the treatment of human MPM.

therapy option for MPM patients who are not candidates for curative-intent surgery (7).

Besides the recent success with the addition of bevacizumab to platinum-based chemotherapy, accumulating preclinical evidence suggests that angiogenesis has a crucial role in MPM progression. For example, high tumor microvessel density (MVD) was shown to be an independent poor prognostic factor in human MPM (8). Moreover, among patients with solid tumors, those with MPM had the highest circulating VEGF levels and these elevated levels were associated with poor clinical outcome (9, 10). In support of this, neutralizing antibodies against either VEGF or its receptors were shown to inhibit MPM cell proliferation *in vitro*, indicating that—besides inducing angiogenesis—VEGF can also support MPM growth in an autocrine manner (9).

In addition to VEGF family members, other angiogenic factors and receptors, including fibroblast growth factors (FGF), FGF receptors (FGFR; refs. 11, 12), platelet-derived growth factors (PDGF), and PDGF receptors (PDGFR; ref. 13), are also expressed in MPM. Accordingly, various angiogenesis inhibitors have been tested in MPM in first-line setting or in pretreated patients. Unfortunately, none of these drugs could provide a significant survival benefit for patients with MPM (14, 15).

Nintedanib (BIBF1120) is a small molecule receptor tyrosine kinase inhibitor (RTKI) of VEGFR 1–3, FGFR 1–3, and PDGFR α/β, as well as members of the Src family (16). The antitumor potential of nintedanib has been demonstrated in preclinical models of liver (17), head and neck (16), renal (16), lung (16, 18), pancreatic (18), colon, ovarian, and prostate cancers (16). Nintedanib has demonstrated clinical activity in ovarian (19) and renal cancers (20) and, moreover, it has been approved in Europe for the second-line treatment of patients with locally advanced, metastatic or locally recurrent lung adenocarcinoma in combination with docetaxel (21). Furthermore, nintedanib was approved in 2014 for use in patients with idiopathic pulmonary fibrosis (22), a devastating lung disease characterized by progressive scarring of the lung parenchyma mediated in part by profibrotic factors including PDGF and FGF. These clinical findings, taken together with the aforementioned preclinical data, provided the rationale for the recent LUME-Meso phase II trial, which demonstrated that the addition of nintedanib to cisplatin/pemetrexed significantly prolongs progression-free survival (PFS) in patients with unresectable MPM (23). Based on the promising phase II data, the LUME-Meso study has been extended and it is currently enrolling patients as a confirmatory phase III trial (24). However, the preclinical anti-MPM activity of nintedanib has not been studied in detail so far. Therefore, in the current study, we evaluated the potential of nintedanib against human MPM cell lines, primary cell cultures, and tumor xenografts.

Materials and Methods

Cell culture

SPC111, SPC212, and M38K cells were established from human biphasic MPMs and kindly provided by Prof. R. Stahel (SPC111 and SPC212, University of Zurich, Zurich, Switzerland) and by Prof. V.L. Kinnula (M38K, University of Helsinki, Helsinki, Finland). The I2 epithelioid MPM cell line was kindly provided by Prof. A. Catania (University of Milano, Milano Italy). p31 (epithelioid MPM) was kindly provided by Prof. K. Grankvist (University of Umea, Umea, Sweden). The VMC and Meso primary cell cultures were established at the Medical University of Vienna. The nonmalignant mesothelial cell line Met5A (ATCC CRL-9444) was purchased from the American Type Culture Collection. The NP normal mesothelial cell cultures were established from pleura tissue samples of patients operated on for spontaneous pneumothorax. Histological subtypes, drug sensitivity data, target RTK copy-number changes, and mutational status of tumor suppressor genes of MPM cell lines are presented in Supplementary Tables S1 and S2. Cells were maintained in RPMI-1640 or DMEM supplemented with 10% fetal calf serum (FCS) (Sigma Chemical Co.), 100 U/mL penicillin and 10 mg/mL streptomycin (Sigma Chemical Co.) and regularly screened for Mycoplasma contamination. Cell line authentication was performed as previously described (12). All cell lines were maintained at 37°C in a humidified incubator with 5% CO_2.

Western blot analysis

MPM cells (2×10^5) were seeded into 6-well plates and incubated with nintedanib or solvent after 24 hours of recovery. Cells were harvested in RIPA buffer containing protease inhibitor cocktail (both from Fisher Scientific), and proteins were separated by SDS-PAGE, blotted onto nitrocellulose membranes, and immunostained with the following primary antibodies (all from Cell Signaling Technology): rabbit polyclonal pErk1/2 (#9101), Erk1/2 (#9102), pAkt (#4058), Akt (#9272), pS6 (#2215), S6 (#2217), β-actin (#4970) at a dilution of 1:1,000, followed by a horseradish peroxidase-coupled secondary antibody and developed by ECL Reagent (GE Healthcare). Films were scanned and phosphorylation was quantified using the ImageJ software.

Orthotopic *in vivo* MPM xenograft model

To establish orthotopically growing tumors, 2×10^6 MPM cells were inoculated into the thoracic cavity of 8-week-old SCID mice. Once (based on our preliminary experiments) MPM nodules reached a macroscopically visible size (28 days after tumor implantation), mice ($n = 9$/group) were randomized into

treatment and control groups. For the survival experiments, animals with human p31 MPM tumors growing in the thoracic cavity received (i) nintedanib *per os* (PO, 50 mg/kg), (ii) nintedanib intraperitoneally (IP, 50 mg/kg), (iii) solvent PO, or (iv) solvent IP. Animals were weighed three times a week and euthanized when they showed significant morbidity. Nintedanib was dissolved either in methylcellulose (PO treatment) or in DMSO (IP treatment).

For the tumor growth experiment, p31 or SPC111 cells were injected intrathoracically as described above. The animals were then randomized into the following groups, each consisting of 10 mice: (i) solvent IP, (ii) cisplatin (3 mg/kg, dissolved in 0.9% NaCl IP) and pemetrexed IP (30 mg/kg, dissolved in 0.9% NaCl), (iii) nintedanib IP (50 mg/kg, dissolved in DMSO), (iv) bevacizumab IP (10 mg/kg), (v) cisplatin and pemetrexed in combination with nintedanib IP, (vi) cisplatin and pemetrexed in combination with bevacizumab IP.

The treatments started 21 and 12 days after p31 and SPC111 tumor cell inoculation, respectively. In both sets of experiments, cisplatin was applied once weekly, pemetrexed and nintedanib were administered five times a week on consecutive days, while bevacizumab was injected twice weekly. Body weight was checked thrice a week. The experiments were terminated on the 28th day (p31 tumors) and 16th day (SPC111 tumors) of treatments due to signs of distress in the control groups. Two hours before the mice were sacrificed, 200 mg/kg BrdUrd in 0.9% NaCl was injected intraperitoneally. Tumor nodules were harvested, weighed, and frozen in liquid nitrogen. All animal experiments were carried out in accordance with the ARRIVE guidelines (25) and with the animal welfare regulations of the host institutes (permission number: PEI/001/2574-6/2015).

Immunohistochemical analysis of xenograft tumors

Consecutive 10-μm-frozen sections were prepared and fixed in methanol (for hematoxylin, CD31, and BrdUrd staining) or 4.5% Histofix (for cleaved caspase-3 staining). For microvessel labeling, the slides were incubated with rat monoclonal anti-mouse CD31 antibody (Clone SZ31, Dianova, dilution 1:50) followed by Alexa 555-conjugated anti-rat IgG (Cell Signaling Technology). To detect apoptotic cells, sections were incubated with cleaved caspase-3 antibody (Cell Signaling, dilution 1:400) and anti-rabbit FITC (Jackson). To determine the proliferation rate of tumor cells, anti-BrdUrd monoclonal antibody (Becton Dickinson, Bioscience, dilution 1:50) and FITC-conjugated anti-mouse IgG (Jackson) were applied. Nuclei were stained with DAPI (Thermo Fisher Scientific). Slides were scanned by TissueFAXS and ImageJ was used to analyze the images as described recently (26). Relative microvessel areas (MVA) were calculated by counting the number of CD31-positive pixels in the total tumor area. The percentages for cleaved caspase-3 and BrdUrd-positive pixels were also determined.

Statistical analysis

Distribution of the data was tested with the Shapiro–Wilk test. For parametric data, *t* test was used when comparing two groups, and one-way ANOVA with Tukey multiple comparison test was used for the comparison of more than two groups. Nonparametric data were analyzed with Mann–Whitney *U* test, and the Kruskal–Wallis test with the Dunn multiple comparison *post hoc* test was used for analyzing more than two groups. The correlations between different parameters were calculated by Spearman correlation test. Kaplan–Meier curves for animals' survival were evaluated and the log-rank test was used to establish the significance of the difference. All statistical analysis was performed by using GraphPad Prism 7.0 software (GraphPad Inc.). *P* values are given as two sided and were considered statistically significant below 0.05.

Details of the procedures that were used for RNA isolation, reverse transcription, real-time PCR, magnetic resonance imaging, array comparative genomic hybridization (array CGH), exome sequencing, ELISA, and *in vitro* chemosensitivity, clonogenic, proliferation, apoptosis, and migration assays can be found in Supplementary Materials and Methods.

Results

Receptor tyrosine kinases (RTK) targeted by nintedanib are coexpressed in MPM cells

Transcript levels of the key molecular targets of nintedanib were determined in 20 MPM cell lines and, as controls, in the Met5a immortalized mesothelial cell line and in three primary mesothelial cell cultures. While PDGFRA, VEGFR1-3, FGFR2, and FGFR3 were expressed only by some of the cell lines and at relatively low levels, PDGFRB and FGFR1 mRNAs could be detected in each tumor cell line and in most of the nonmalignant control cell lines, although with various expression levels (Fig. 1A). Importantly, all of the MPM cell lines were double positive for PDGFRB and FGFR1. Moreover, FGFR1 expressions were elevated in MPM cells compared with control mesothelial cells (Fig. 1A; $P < 0.05$). The copy-number changes of *PDGFRA*, *PDGFRB*, *VEGFR2*, and *FGFR1* are shown in Supplementary Table S1. The mutations identified in tumor suppressor genes *BAP1*, *NF2*, and *CDKN2A* are presented in Supplementary Table S2. Notably, none of these data were associated with nintedanib sensitivity (raw data are shown in Supplementary Tables S1 and S2). The mRNA levels of PDGFRB and FGFR1 in MPM cells according to their histological subtypes are shown in Supplementary Fig. S1. Neither these two RTKs (Supplementary Fig. S1) nor the other target receptors (data not shown) exhibited a histotype-specific expression profile. While sarcomatoid and biphasic MPM cells showed similar expression patterns, the epithelioid group was more heterogeneous.

Nintedanib inhibits *in vitro* MPM growth

Mesothelial and MPM cells were exposed to different concentrations of nintedanib for 72 hours. Cell viability was determined by SRB assay, dose–response curves were plotted to determine IC_{50} values for each cell line. IC_{50} values for the Met5a and NP3 control cell lines were 1.1 and 4.1 μmol/L, respectively. MPM cells showed a wide range of sensitivity with IC_{50} varying from 1.6 to 5.9 μmol/L, with no association to histological subtype (Fig. 1B; Supplementary Table S1) or mRNA expression profile of the target RTKs (data not shown). In long-term growth assays, where MPM cells were treated with nintedanib for 10 days, nintedanib was able to effectively inhibit clonogenicity at much lower concentrations (Fig. 1C).

Because RTKs targeted by nintedanib were shown to interfere with chemotherapy in other malignancies (27–29), we next analyzed whether nintedanib has an impact on chemosensitivity in two different human MPM cell lines, the p31 and SPC111. SPC111 cells are more resistant to nintedanib than p31 cells

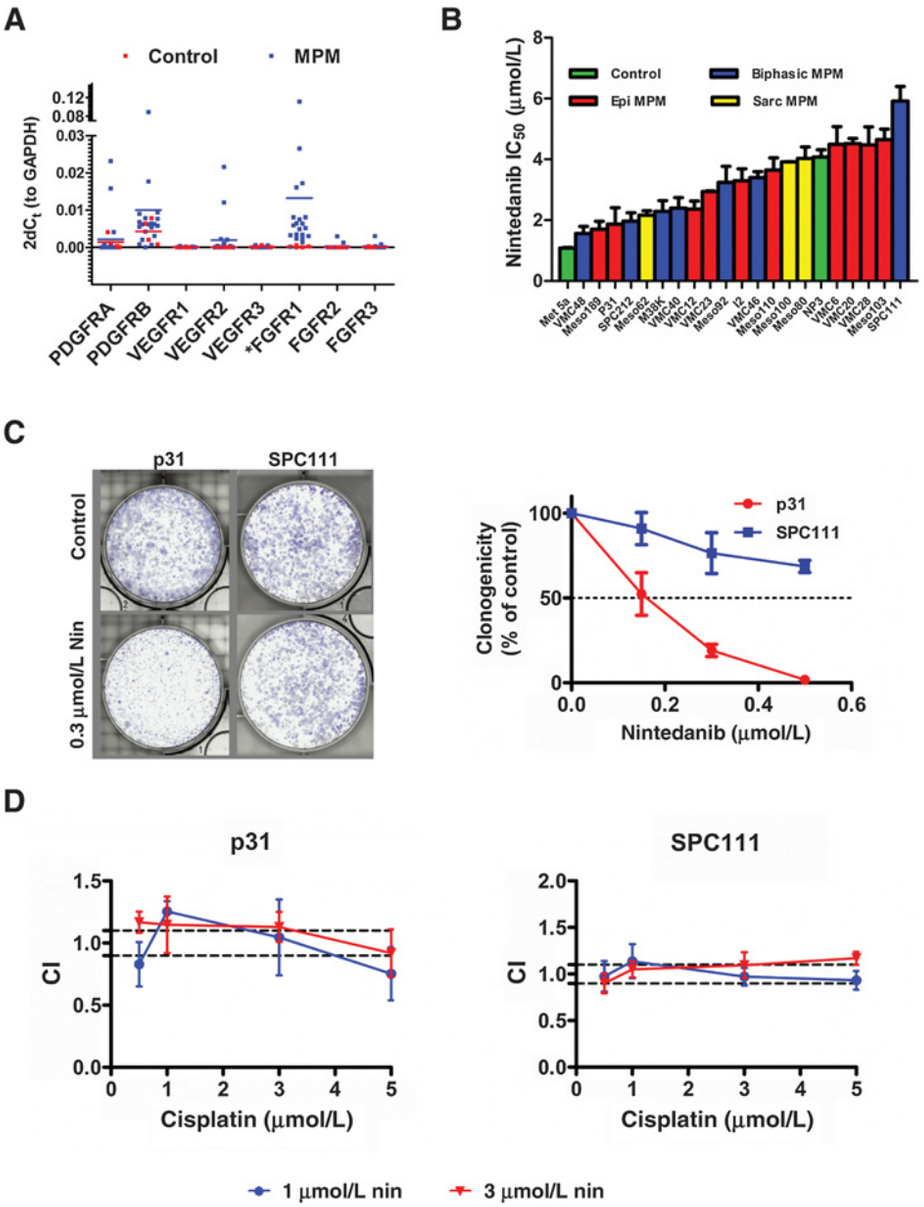

Figure 1.
Target RTKs of nintedanib in nonmalignant mesothelial and in MPM cells and the *in vitro* inhibitory effect of nintedanib on MPM growth as a single agent and also in combination with chemotherapy. **A,** mRNA levels of PDGFRA and -B, VEGFR1-3, and FGFR1-3 in three normal mesothelial cell lines (red dots), in the immortalized Met5A cell line (red dots) and in MPM cells (blue dots; $n = 20$). Horizontal lines represent mean. FGFR1 mRNA levels are significantly higher in the MPM cell lines (*, $P < 0.05$ vs. controls). **B,** MPM cells were treated with different concentrations of nintedanib and incubated for 72 hours. Viability was determined with SRB assay. IC_{50} values of control mesothelial ($n = 2$) and MPM cells ($n = 20$) with different histological subtypes are shown as mean + SD. Colors green, red, blue, and yellow indicate control mesothelial, epithelioid, biphasic, and sarcomatoid MPM cells, respectively. **C,** For clonogenic survival analysis, MPM cells were seeded at low densities, treated with different concentrations of nintedanib, and incubated for 10 days. Crystal violet was dissolved and intensity was quantified to determine clonogenicity (representative examples are shown on the left). Data (mean ± SD) from three independent experiments are shown on the right. **D,** To investigate drug interactions with chemotherapy, P31 and SPC111 cells were treated with different concentrations of nintedanib and cisplatin alone or in combination. Viabilities after 72 hours were measured with SRB assay and combination indices were calculated. CI values <0.9, from 0.9 to 1.1, or >1.1 represent synergism, additive effects or antagonism between nintedanib and cisplatin, respectively. Data (mean ± SD) from three independent experiments are shown.

(IC_{50}s are 5.9 vs. 1.9 μmol/L, respectively; Supplementary Table S1). With respect to their cisplatin sensitivity, p31 is more resistant than SPC111 (IC_{50}s are 4.3 vs. 0.7 μmol/L, respectively; Supplementary Table S1). FGFR1 expression levels are similar in the two cell lines, while PDGFRB transcript levels are higher in p31 cells. The other target RTKs of nintedanib cannot be detected on mRNA level in either cell lines (Supplementary Fig. S2). Notably, at certain concentrations, we observed an additive effect between nintedanib and the established chemotherapeutic agent (cisplatin) in both cell lines (Fig. 1D). However, no synergism between nintedanib and cisplatin was evident in p31 and SPC111 cells (Fig. 1D) and, furthermore, there was no correlation between cisplatin and nintedanib sensitivities in a panel of 20 human MPM cell lines (raw data are shown in Supplementary Table S1).

In vitro effects of nintedanib on MPM cell proliferation, migration, and apoptosis and on the downstream signaling of its target receptors

BrdUrd incorporation assay was performed in five different MPM cell lines to investigate the effect of nintedanib on tumor cell proliferation. The drug exhibited a significant antiproliferative effect in each MPM cell line in a dose-dependent manner (Fig. 2A).

To study apoptosis induction, TUNEL assays were performed (Fig. 2B), which enable the detection of DNA fragmentation during apoptosis. Significantly elevated apoptosis rates upon nintedanib treatment could be confirmed only in SPC212 and VMC40 cells (Fig. 2B).

To study the antimigratory activity of nintedanib, five human MPM cell lines with different sensitivities to the drug (Supplementary Table S1) were used. Nintedanib treatment (1 or

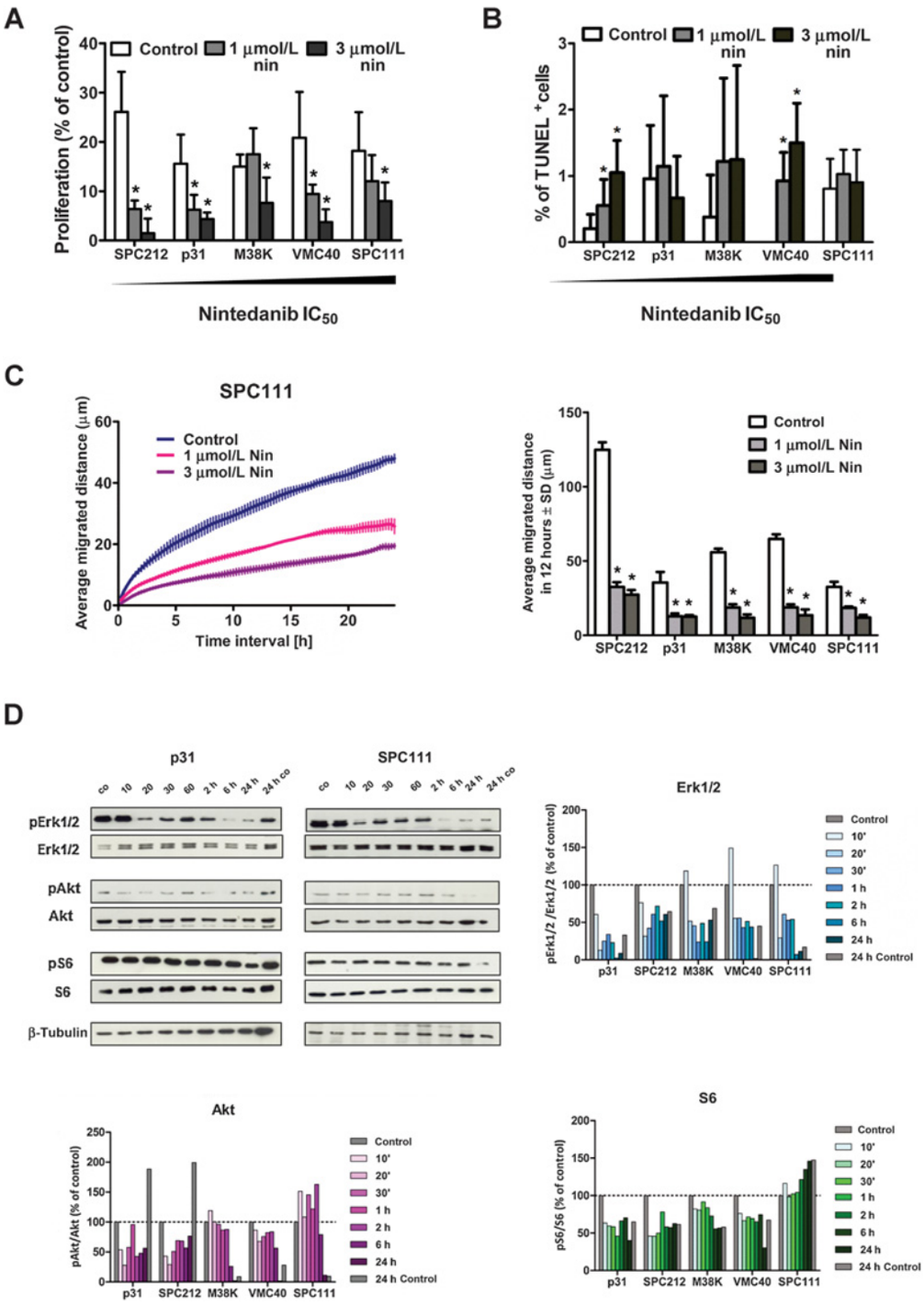

Figure 2.

Impact of nintedanib on *in vitro* proliferation, apoptosis, and migration of MPM cells. **A,** MPM cells were treated with nintedanib for 48 hours and the proliferation rate was measured by BrdUrd assay. Significant reduction of cell proliferation could be observed upon nintedanib treatment in all five MPM cultures. Columns, mean for three experiments; bars, SD. *, $P \leq 0.05$. **B,** To measure the ratio of apoptotic cells in MPM cultures, TUNEL staining was performed on the SPC212, P31, M38K, VMC40, and SPC111 cultures exposed for 48 hours to increasing concentrations of nintedanib. Columns, mean for three experiments; bars, SD. *, $P \leq 0.05$. **C,** MPM cell cultures were treated with nintedanib (1 or 3 μmol/L) or solvent in CO_2-independent medium with 10% FBS over 24 hours and cell migration was analyzed with videomicroscopy. Nintedanib showed a significant antimigratory potential at both concentrations after 12 hours of treatment (*, $P \leq 0.0001$ vs. control, left). Average distance SPC111 cells migrated during various time periods are plotted on the right. **D,** Time-course Western blot assays evaluating the effect of 0.5 μmol/L nintedanib treatment on Erk1/2, Akt, and S6 phosphorylation in P31, SPC212, M38K, VMC40, and SPC111 cells. Scanned films of p31 and SPC111 cells are presented, densitometric quantification of phosphorylation in all five cell lines are shown in bar graphs. Beta-tubulin was used as loading control.

3 μmol/L) was able to significantly reduce the migratory activity of each cell line. Average displacements of SPC111 cells are plotted, for various elapsed time periods, in Fig. 2C. Time-lapse microscopy demonstrating the effect of nintedanib treatment on the migratory activity of the SPC212 cells is shown in Supplementary Video S1.

Time-course experiments on nintedanib's effects on Erk, Akt, and S6 phosphorylation were carried out to investigate the molecular mechanisms behind the antitumor effects of the drug. MPM cells were exposed to 0.5 μmol/L nintedanib for different times ranging from 5 minutes to 24 hours. Activation of the abovementioned proteins was determined by Western blot analysis. As shown in Fig. 2D; Supplementary Fig S3, the phosphorylation of Erk1/2 was efficiently blocked as early as 20 minutes in each cell line. Probably due to changes in cell density and in growth factor concentrations, Erk activation declined during the 24-hour incubation also in the solvent controls. Nevertheless, the inhibition of Erk phosphorylation was apparent in p31 and VMC40 cells even at this later time point. Only a minor inhibitory effect was seen in SPC111 and M38K cells, while no effect was observable in SPC212 cells. Regarding Akt phosphorylation, an inhibitory effect could be observed in p31, SPC212, M38K, and VMC40 cells, although in the latter two cell lines only at later time points (24 hours). Nintedanib (at 0.5 μmol/L) had no effect on the activation of Akt in the SPC111 cells, which was the most nintedanib-resistant cell line in the whole panel. The drug's impact on S6 phosphorylation was negligible.

Nintedanib inhibits human MPM growth *in vivo* and prolongs survival of mice bearing orthotopic human MPM xenografts

To examine the *in vivo* efficacy of nintedanib, we used an orthotopic MPM model where human p31 or SPC111 MPM cells were injected into the thoracic cavity of SCID mice.

In the first set of these experiments, 50 mg/kg nintedanib was administered either PO or IP, starting from the 21st day after inoculation of p31 cells. Based on our preliminary experiments (data not shown), by this time, several tumor nodules are already visible macroscopically on the pleura of mice. The p31 cells highly express PDGFRB and FGFR1 receptors (Supplementary Fig. S2), they are relatively responsive to nintedanib (Fig. 1) but insensitive to cisplatin (Supplementary Table S1). Nintedanib was well tolerated without any signs of toxicity during the treatment period. Survival of PO-treated animals showed a favorable trend, but no significant benefit ($P = 0.059$ vs. PO control; Fig. 3A). However, nintedanib significantly prolonged the survival of mice when it was administered IP ($P = 0.0008$; Fig. 3A). Importantly, nintedanib IP also significantly inhibited the relative weight loss of the animals ($P = 0.0337$; Fig. 3B), in accordance with their better overall condition at the end of the experiment. Our interpretation of these data is that nintedanib IP not only prolongs the survival of mice with orthotopically growing human MPM tumors but also interferes with MPM-induced cachexia. To further corroborate the antitumor effects of nintedanib, *in vivo* MPM growth was also examined by MR imaging. Although control animals had significant intrathoracic tumor burdens on day 25 after tumor implantation, a marked reduction of tumor mass in nintedanib-treated animals was evident (Fig. 3C).

In the second set of orthotopic MPM xenograft experiments, the addition of nintedanib to standard-of-care chemotherapy was investigated by implanting two different human MPM cell lines, the p31 and the SPC111 (Fig. 4). Nintedanib was administered IP, as in the aforementioned set of *in vivo* experiments, this route of administration proved to be more effective than PO treatment. We could demonstrate significantly reduced tumor burden in mice treated with cisplatin/pemetrexed chemotherapy alone or nintedanib alone in both cell models when compared with untreated controls (Fig. 4A). In comparison with untreated control tumors, combined chemo- and antiangiogenic regimens (including either nintedanib or bevacizumab) also exhibited significant *in vivo* tumor growth-inhibitory potential in both cell models (Fig. 4A). Importantly, in accordance with a previous study from Li Q and colleagues (30), bevacizumab alone was effective only against p31 tumors with high baseline VEGF-A levels (vs. control) and could not provide therapeutic benefit in the SPC111 model where tumor cells had markedly low baseline VEGF-A levels, as measured by ELISA (Fig. 4A and B).

Another key observation in this second set of *in vivo* experiments was that adding nintedanib to standard chemotherapy produces significantly higher responses than chemotherapy alone. These responses were comparable (P31 tumors) or superior (SPC111 tumors) to those achievable by combined bevacizumab and chemotherapy (Fig. 4A). It is also important to mention here that unlike bevacizumab alone, nintedanib alone proved to be a more effective inhibitor of *in vivo* MPM growth than standard chemotherapy in p31 tumors with higher baseline VEGF-A expression (Fig. 4A and B).

Nintedanib effectively blocks angiogenesis in orthotopically growing human MPM xenografts independently of baseline VEGF-A expression

Morphometric analysis using CD31 as an endothelial marker revealed a strong tendency for increased microvessel areas (MVAs) in control p31 tumors with high baseline VEGF-A expression as compared with MVAs in untreated low baseline VEGF-A SPC111 tumors (2.7% ± 1.2% vs. 1.2% ± 0.8%, respectively; $P = 0.067$). In line with the potent *in vivo* MPM growth inhibitory effect of nintedanib, significantly lower MVAs were present in tumors treated with nintedanib (alone or in combination with chemotherapy) in both cell models (vs. controls; Fig. 5A). Interestingly though, we did not observe a significant reduction in MVAs of p31 or SPC111 tumors treated with bevacizumab with or without chemotherapy (Fig. 5A). The potent antivascular effect of nintedanib was accompanied by increased intratumoral necrosis in both cell models. This was most prominent in the combined nintedanib/chemotherapy groups (Fig. 5B). Nintedanib as a single agent resulted in significantly increased MPM cell apoptosis ($P = 0.0317$; vs. control; Fig. 5C) and decreased proliferation in p31 tumors ($P = 0.0341$ vs. control; Fig. 5D). However, none of the other treatment groups showed significant changes in tumor cell apoptosis and proliferation rates and, furthermore, we failed to identify any obvious associations between these parameters (i.e., MPM cell apoptosis and proliferation) and the net *in vivo* tumor growth inhibitory effect of nintedanib presented in Fig. 4.

Discussion

The current first-line systemic standard-of-care therapy for MPM is cisplatin plus pemetrexed. The recent phase III MAPS trial demonstrated that the median OS of unresectable MPM patients from adding bevacizumab to this chemotherapeutic regimen can be increased from 16.1 to 18.8 months (6), indicating that angiogenesis inhibition might be an effective anti-MPM

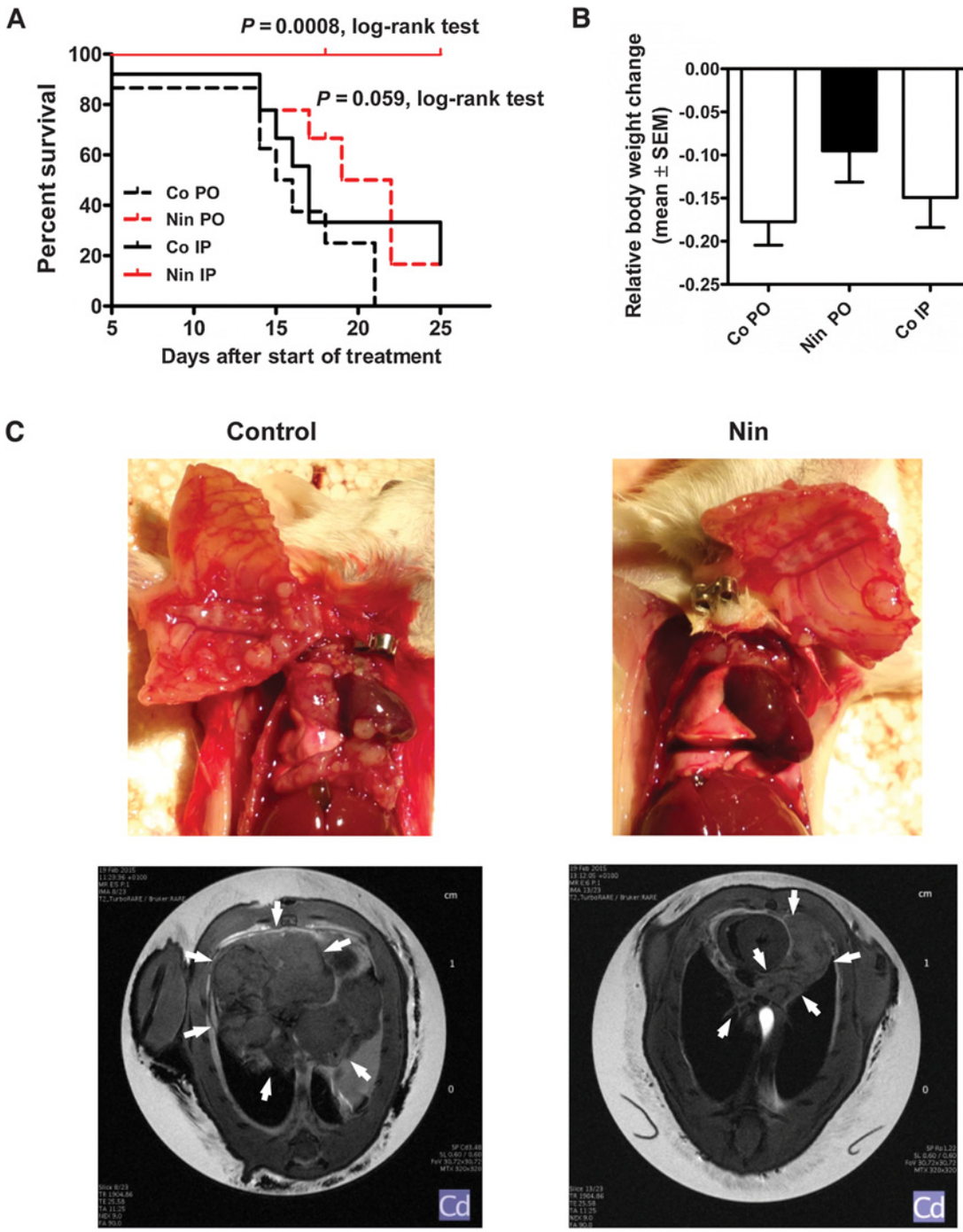

Figure 3.

Nintedanib prolongs survival of mice bearing orthotopically growing human MPM. Human p31 MPM cells, which express relatively high levels of PDGFRB and FGFR1, were injected orthotopically into SCID mice. Nintedanib was administered from day 28 after tumor inoculation, when small tumor nodules were already visible on the pleura. **A,** Kaplan–Meier curves for the survival of human MPM-bearing mice treated with nintedanib, according to the route of drug administration. Animals treated with nintedanib IP had significantly longer survival times than those treated with vehicle IP only ($P = 0.0008$). **B,** Relative body weight changes of human MPM-bearing mice. *, $P = 0.0337$, versus IP controls. **C,** Representative macroscopic (top) and MR (bottom) images of orthotopically growing human MPM tumors (25th day of treatment period) in control and nintedanib (IP) treated mice. In MR images, arrows mark the tumor rims.

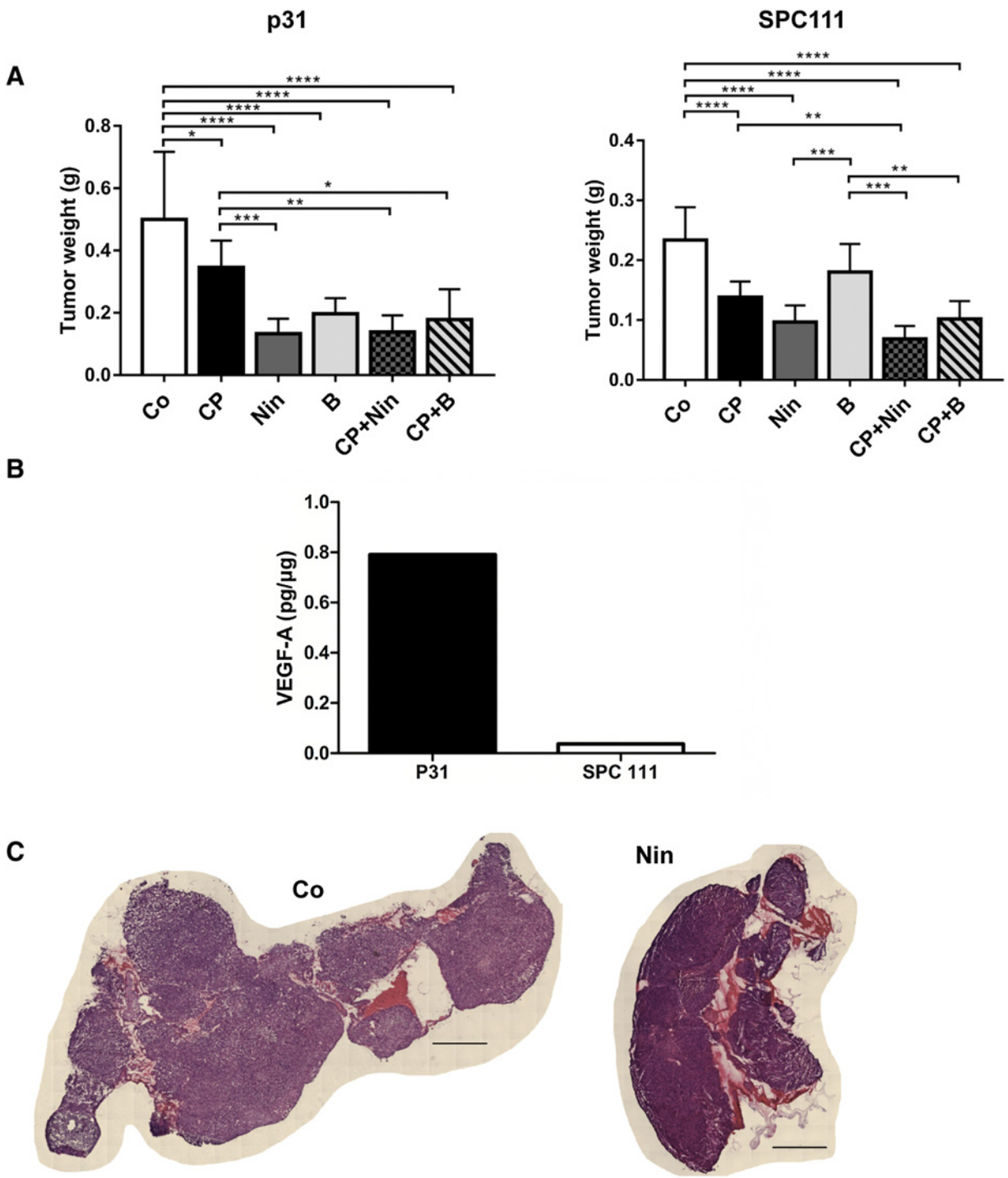

Figure 4.

Nintedanib inhibits the growth of orthotopically growing human MPM. **A,** Effects of different single or combined chemo- and antiangiogenic therapies on *in vivo* MPM growth. Twenty-eight days (p31; left) and 12 days (SPC111; right) after tumor implantations, the following IP therapies were applied: (i) solvent (control), (ii) cisplatin + pemetrexed (CP), (iii) nintedanib alone (Nin), (iv) bevacizumab alone (B), (v) cisplatin/pemetrexed and nintedanib (CP + Nin), (vi) cisplatin/pemetrexed and bevacizumab (CP + B). Total tumor weight of p31 (left) and SPC111 (right) xenografts in each mouse was determined. Columns, means for 10 mice per group; bars, SD; *, $P \leq 0.05$; **, $P \leq 0.005$; ***, $P \leq 0.0005$; ****, $P \leq 0.0001$. **B,** ELISA detection of secreted VEGF-A in conditioned medium from p31 and SPC111 cell cultures. **C,** Micrographs of representative hematoxylin and eosin–stained p31 tumor sections. Scale bars, 1 mm.

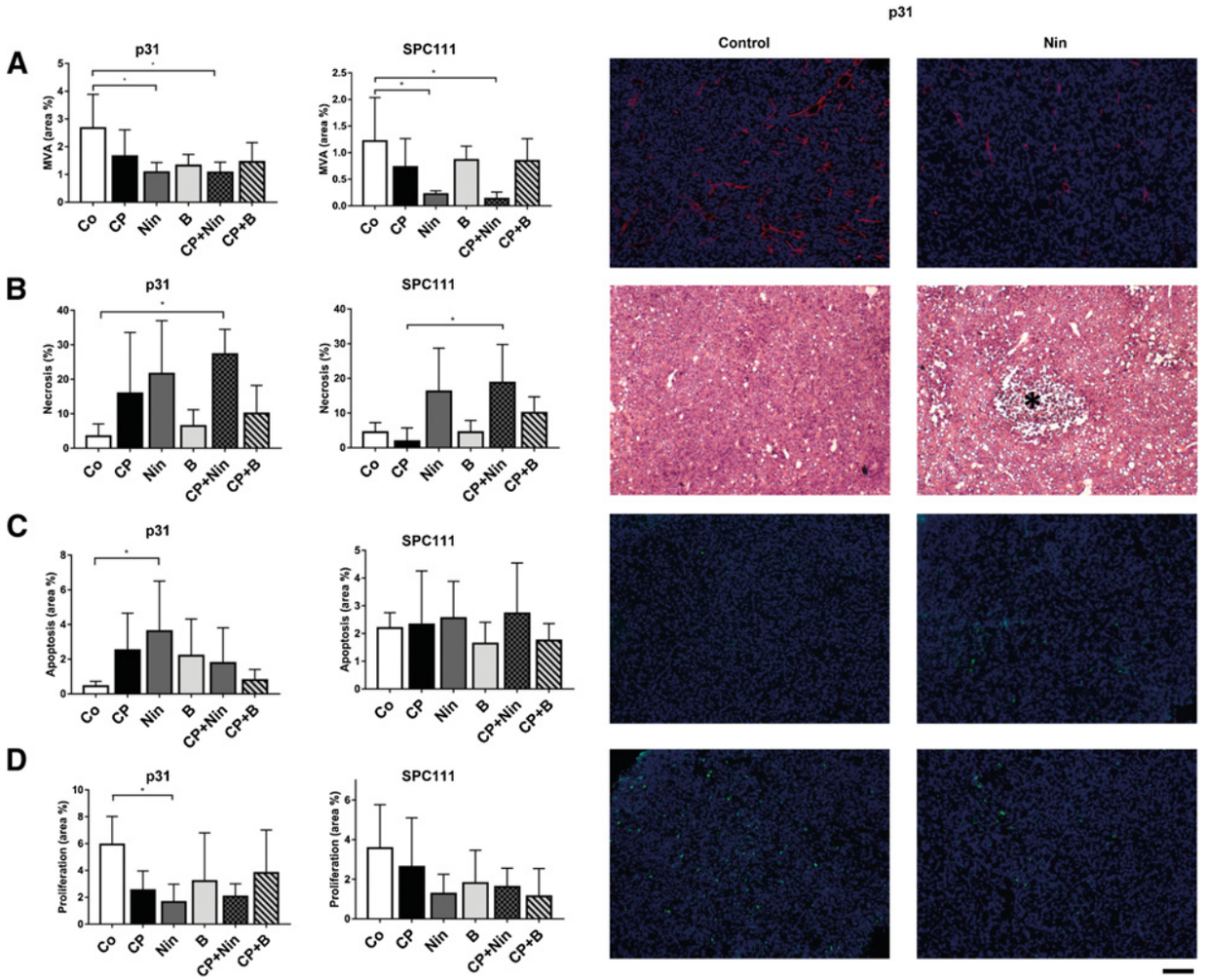

Figure 5.

Antivascular and antitumor effects of nintedanib and bevacizumab as single agents or in combination with standard-of-care chemotherapy in orthotopically growing p31 and SPC111 MPM xenografts. MVAs (CD31-positive areas per total areas) and percentages of necrotic tumor regions and the ratios of apoptotic and proliferating MPM cells were determined across the entire areas of p31 and SPC111 tumor sections. **A,** Graph (left) of MVAs in p31 and SPC111 tumors. Representative images (right) of frozen p31 tissue sections labeled with the endothelial marker CD31 (red) and with DAPI (as nuclear counterstain; blue). Columns, means for 10 mice per group; bars, SD; *, $P \leq 0.05$ versus control. **B,** Graph (left) of necrotic area ratios in p31 and SPC111 tumors. Necrotic area ratios are shown in the percentage of the total tumor section. Columns, means for 10 mice per group; bars, SD; *, $P \leq 0.05$. Representative H&E images of control versus nintedanib-treated p31 tumors are shown on the right. Asterisk marks necrotic area. **C,** Graph (left of MPM cell apoptosis in p31 and SPC111 xenografts. Representative images of control versus nintedanib-treated p31 tumors are shown on the right. Caspase-3 cleavage (i.e., apoptosis) was detected *in situ* by immunofluorescence. The apoptotic rate is expressed as the percentage of cleaved caspase-3–positive cells (green). Nuclei are counterstained with DAPI (blue). Columns, means for 10 mice per group; bars, SD; *, $P \leq 0.05$. **D,** Graph (left) of MPM cell proliferation in p31 and SPC111 xenografts. Representative images of control versus nintedanib-treated p31 tumors are shown on the right. The ratio of proliferating MPM cells was assessed by BrdUrd labeling (green). Nuclei are counterstained with DAPI (blue). Columns, means for 10 mice per group; bars, SD; *, $P \leq 0.05$; scale bar, 100 μm; Co, control; CP, cisplatin/pemetrexed; Nin, nintedanib; B, bevacizumab; CP + Nin, cisplatin/pemetrexed and nintedanib; CP + B, cisplatin/pemetrexed and bevacizumab.

strategy and, accordingly, that additional antiangiogenic agents need to be evaluated in human MPM.

Here, by utilizing different *in vitro* and *in vivo* models of human MPM, we examined the antitumor activity of nintedanib, a small molecule RTKI targeting VEGFR 1–3, FGFR 1–3, and PDGFR α/β signaling (16). Although the biological impact of these angiogenic pathways has already been reported in MPM, this is the first preclinical study investigating the therapeutic efficacy of nintedanib in this malignancy.

First, we show that all of the studied 20 MPM cell lines express relatively high FGFR1 and PDGFRB levels. PDGFRA and VEGFR2 expressions were also detected in certain cell lines while the mRNA levels of other nintedanib target RTKs were rather low or absent. This is in line with previous studies of our group and others (12, 13, 31). Further corroborating the role of PDGFRA and VEGFR2 signaling in MPM, a recent retrospective study analyzing tumor samples of advanced-stage MPM cases revealed that one-third of the patients carried mutations of nintedanib target genes

(32), although these findings have not been confirmed in other MPM genomics studies (33, 34).

Production of FGFR, PDGFR, and VEGFR ligands might enable MPM cells to promote their own growth and survival *via* distinct autocrine signaling loops. In support of this, Strizzi and colleagues showed that VEGF induces *in vitro* MPM growth *via* the phosphorylation of VEGFR1-2 (9). In the same study, members of the VEGF/VEGFR axis were found to be expressed in human MPM tissue and treatment of MPM cells with neutralizing antibodies against VEGF or VEGFR2 resulted in decreased tumor cell proliferation (9). There is also a substantial volume of literature on the autocrine growth-promoting effects of PDGF/PDGFR and FGF/FGFR pathways in MPM (11–13) and in other solid tumors as well (35). These reports, together with our observation that nintedanib dose-dependently inhibits *in vitro* MPM growth, allow us to conclude that—besides its antiangiogenic potential—nintedanib has a direct *in vitro* anti-MPM effect.

We have reported recently that MPM cells exhibit an exceedingly high migratory potential, even when compared with malignant cells of highly metastatic tumors such as lung cancer or melanoma (36). Studies examining the regulation of MPM cell chemotaxis have shown that the PDGF/PDGFR axis promotes MPM cell migration *via* Erk and PI3 kinase/Akt signaling (37, 38) and, furthermore, that activation of FGFR1 by FGF2 induces MPM cell migration and Erk activation (12). In the current study, we found that nintedanib potently blocks MPM cell migration. In line with this, nintedanib rapidly inhibited the phosphorylation of Erk in all the five investigated MPM cell lines and, moreover, decreased the activation of Akt in those MPM cell lines that were found to be relatively sensitive in the *in vitro* viability assays. Of note, nintedanib has also been shown to inhibit the migration of fibroblasts in idiopathic pulmonary fibrosis (39).

Previous studies from our group and others have reported that FGFR1 blockade enhances the effect of chemotherapy in MPM (12) and in other malignancies (e.g., in breast cancer; ref. 40). Also, PDGFR targeting has been shown to synergize with paclitaxel and doxorubicin in breast cancer *in vitro* and *in vivo* (28). Moreover, copy-number gains of *VEGFR2* induced platinum resistance in lung cancer cells that could be reduced by knocking down VEGFR2 signaling by using small interfering RNA (27). In this study, we observed an additive effect between nintedanib and cisplatin in human MPM cells *in vitro*.

As for the *in vivo* anti-MPM potential of nintedanib, we demonstrated that upon IP administration, the drug significantly prolongs the survival and reduces body weight loss of mice bearing orthotopic human MPM xenografts. Interestingly, although animals treated with nintedanib PO also had longer survival times, this tendency did not reach statistical significance. One possible explanation for this difference is that IP administration of nintedanib results in higher intrathoracic drug concentrations. In support of this, the peritoneal and the thoracic cavities have been reported to be directly connected *via* the lymphatic capillary system of the diaphragm in both mice and humans (41, 42). Although the mechanism and efficacy of this potential transdiaphragmal drug transfer need to be further investigated, chances are that although nintedanib is an orally available and approved drug, in MPM it might exert a more potent antitumor effect when administered IP.

Based on the above-described considerations, in the further combination experiments, both nintedanib and chemotherapy were applied IP. Perhaps, the most striking findings of this second set of animal experiments were that there is a significant efficacy advantage in combining standard chemotherapy with nintedanib, that nintedanib and bevacizumab have comparable *in vivo* anti-MPM potential in tumors with high baseline VEGF-A expression and, moreover, that nintedanib is superior to bevacizumab in human MPM growth inhibition in tumors with low baseline VEGF-A expression. Our data, thus, suggest that nintedanib is as effective as bevacizumab, the reference angiogenesis inhibitor in clinical practice (7, 43), in human MPM xenografts with high baseline VEGF-A expression. Moreover, we also conclude that from the efficacy perspective, nintedanib in combination with chemotherapy can be considered as the preferred antiangiogenic regimen of choice for patients with tumors expressing low VEGF-A levels. This is in accordance with a previous study from Li Q and colleagues who demonstrated that bevacizumab inhibited the orthotopic growth of EHMES-10 MPM cells with high baseline VEGF-A expression but not that of "VEGF–low-producing" MSTO-211H MPM cells (30). However, it has to be kept in mind that baseline VEGF levels detected in our MPM cell lines may have changed during *in vivo* tumor development and, moreover, that the clinical translation of these results is also hampered by the lack of VEGF-A related or other biomarkers that have been validated in patients with MPM or other solid tumors to predict antiangiogenic treatment efficacy (44). Nevertheless, in further support of the more potent antiangiogenic and antitumor activity of nintedanib, we observed significantly reduced vascularization in nintedanib-treated tumors (vs. controls, with or without concurrent chemotherapy and formed by both p31 and SPC111 lines), but not in the bevacizumab-treated p31 or SPC111 tumors. Yet, it is noteworthy that there was a strong tendency for reduced vascularization in bevacizumab-treated p31 tumors with high baseline VEGF-A levels.

The abovementioned findings, taken together with our observation that the IC_{50} values established in most of our *in vitro* assays correspond to higher drug levels than pharmacologically achievable nintedanib tissue concentrations in mammals (i.e., 200–450 nmol/L (16)), suggest that the key component of nintedanib's *in vivo* effect is its antivascular potential. In further support of this, our previous study revealed nintedanib IC_{50} values in endothelial cultures about one order of magnitude lower than the IC_{50}s reported in the present study for MPM cells (16). It is important to mention here, though, that the antivascular and direct antitumor effects of antiangiogenic RTKIs might have partly opposing impacts on tumor progression. As we have reported recently, because antiangiogenic RTKIs destroy the tumor microvasculature, blood capillaries get separated by longer distances resulting in inadequate tumor tissue RTKI penetration and thus limited drug delivery to RTK-expressing tumor cells (26).

We also demonstrate in this study that nintedanib is similarly active in human MPM xenografts as a single agent and in combination with cisplatin/pemetrexed, indicating that—although they can have additive effects *in vitro*—the addition of nintedanib to chemotherapy does not provide a further *in vivo* MPM growth inhibitory effect. In accordance with our current data, Awasthi and colleagues showed that while nintedanib synergizes with gemcitabine in pancreatic cancer *in vitro* and exhibits potent antitumor effect *in vivo*, combined nintedanib/gemcitabine therapy does not provide synergistic tumor growth reduction in mice bearing human pancreas cancer xenografts (35).

It is currently not clear whether and how antiangiogenic drugs can improve the delivery of chemotherapy. According to the

"vessel normalization theory" of Jain and colleagues, bevacizumab "normalizes" the chaotic tumor vasculature and thus increases chemotherapeutic drug delivery (45). However, recent clinical data raised serious concern that bevacizumab reduces, rather than improves, chemotherapy uptake by solid tumors (46). Also in contrast to the vessel normalization concept, Kutluk-Cenik and colleagues reported decreased capillary pericyte coverage and doxorubicin delivery in human pancreatic cancer xenografts following nintedanib therapy (18). One can also assume, therefore, that antiangiogenic RTKIs—which (in contrast to bevacizumab) are typically approved as monotherapies in the clinic (e.g., in renal and liver cancers)—may not promote normalization but, instead, might destabilize the vasculature and thus interfere with drug delivery by destroying the pericyte coverage of the tumor capillaries. This is because the PDGF/PDGFR axis is crucial for pericytes and the pericyte layer has a key role in the maintenance of vessel wall stability (45). In other studies, however, nintedanib "normalized" the vasculature in human A549 lung cancer xenografts (47) and also in an *in vivo* model of pulmonary fibrosis (48).

In summary, our current study provides evidence that nintedanib's target RTKs are (co)expressed in MPM cells and that this triple angiokinase inhibitor inhibits MPM growth and migration *in vitro*. Moreover, our data suggest that nintedanib exhibits potent VEGF-A expression-independent MPM growth inhibition *in vivo* thereby prolonging the survival of MPM-bearing animals. These preclinical findings support the concept of the LUME-Meso trial evaluating nintedanib in combination with cisplatin/pemetrexed in patients with unresectable MPM.

Disclosure of Potential Conflicts of Interest

B. Hegedus and B. Dome report receiving commercial research support from Boehringer-Ingelheim. No potential conflicts of interest were disclosed by the other authors.

Authors' Contributions

Conception and design: V. Laszlo, T. Klikovits, M. Grusch, F. Hilberg, B. Hegedus, B. Dome

Development of methodology: V. Laszlo, J. Tovari, B. Hegedus, B. Dome

Acquisition of data (provided animals, acquired and managed patients, provided facilities, etc.): V. Laszlo, Z. Valko, I. Kovacs, M.A. Hoda, T. Klikovits, D. Lakatos, A. Stiglbauer, M. Groger, C. Pirker, W. Berger, B. Hegedus

Analysis and interpretation of data (e.g., statistical analysis, biostatistics, computational analysis): V. Laszlo, Z. Valko, J. Ozsvar, M.A. Hoda, T. Klikovits, A. Czirok, T. Garay, M. Groger, J. Tovari, C. Pirker, W. Berger, F. Hilberg, B. Hegedus, B. Dome

Writing, review, and/or revision of the manuscript: V. Laszlo, M.A. Hoda, T. Klikovits, A. Czirok, T. Garay, A. Stiglbauer, T.H. Helbich, C. Pirker, M. Grusch, W. Berger, F. Hilberg, B. Hegedus, B. Dome, W. Klepetko

Administrative, technical, or material support (i.e., reporting or organizing data, constructing databases): V. Laszlo, M.A. Hoda, T. Klikovits, T. Garay, B. Hegedus

Study supervision: V. Laszlo, M. Grusch, B. Hegedus, B. Dome

Acknowledgments

This work was supported by Boehringer Ingelheim RCV GmbH, Vienna, Austria, the Herzfelder Family Foundation, the Initiative for Cancer Research of the Medical University of Vienna and from the Austrian National Bank (OeNB, 16912), (M. Grusch), the Hungarian National Research, Development and Innovation Office (AIK 12-1-2013-0041, K109626, K108465, KNN121510 and SNN114490, B. Dome; K116295, 16-1-2017-0439, J. Tovari), the Semmelweis University Start-Up grant (40148-11658, B. Dome), the Austrian Science Fund (I2872, B. Hegedus), and the Vienna Fund for Innovative Interdisciplinary Cancer Research (B. Dome). T. Garay is the recipient of a postdoctoral fellowship of the Hungarian Academy of Sciences.

The authors thank the excellent technical assistance of Barbara Dekan.

The costs of publication of this article were defrayed in part by the payment of page charges. This article must therefore be hereby marked *advertisement* in accordance with 18 U.S.C. Section 1734 solely to indicate this fact.

Received May 26, 2017; revised February 22, 2018; accepted April 26, 2018; published first May 3, 2018.

References

1. Carbone M, Kratzke RA, Testa JR. The pathogenesis of mesothelioma. Semin Oncol 2002;29:2–17.
2. Testa JR, Cheung M, Pei J, Below JE, Tan Y, Sementino E, et al. Germline BAP1 mutations predispose to malignant mesothelioma. Nat Genet 2011;43:1022–5.
3. Corson JM. Pathology of diffuse malignant pleural mesothelioma. Semin Thorac Cardiovasc Surg 1997;9:347–55.
4. Finn RS, Brims FJ, Gandhi A, Olsen N, Musk AW, Maskell NA, et al. Postmortem findings of malignant pleural mesothelioma: a two-center study of 318 patients. Chest 2012;142:1267–73.
5. Vogelzang NJ. Chemotherapy for malignant pleural mesothelioma. Lancet 2008;371:1640–2.
6. Zalcman G, Mazieres J, Margery J, Greillier L, Audigier-Valette C, Moro-Sibilot D, et al. Bevacizumab for newly diagnosed pleural mesothelioma in the Mesothelioma Avastin Cisplatin Pemetrexed Study (MAPS): a randomised, controlled, open-label, phase 3 trial. Lancet 2016;387:1405–14.
7. Ettinger DS, Wood DE, Akerley W, Bazhenova LA, Borghaei H, Camidge DR, et al. NCCN guidelines insights: malignant pleural mesothelioma, version 3.2016. J Natl Compr Canc Netw 2016;14:825–36.
8. Kumar-Singh S, Vermeulen PB, Weyler J, Segers K, Weyn B, Van Daele A, et al. Evaluation of tumour angiogenesis as a prognostic marker in malignant mesothelioma. J Pathol 1997;182:211–6.
9. Strizzi L, Catalano A, Vianale G, Orecchia S, Casalini A, Tassi G, et al. Vascular endothelial growth factor is an autocrine growth factor in human malignant mesothelioma. J Pathol 2001;193:468–75.
10. Yasumitsu A, Tabata C, Tabata R, Hirayama N, Murakami A, Yamada S, et al. Clinical significance of serum vascular endothelial growth factor in malignant pleural mesothelioma. J thorac Oncol 2010;5:479–83.
11. Kumar-Singh S, Weyler J, Martin MJ, Vermeulen PB, Van Marck E. Angiogenic cytokines in mesothelioma: a study of VEGF, FGF-1 and -2, and TGF beta expression. J Pathol 1999;189:72–8.
12. Schelch K, Hoda MA, Klikovits T, Munzker J, Ghanim B, Wagner C, et al. Fibroblast growth factor receptor inhibition is active against mesothelioma and synergizes with radio- and chemotherapy. Am J Respir Crit Care Med 2014;190:763–72.
13. Langerak AW, De Laat PA, Van Der Linden-Van Beurden CA, Delahaye M, Van Der Kwast TH, Hoogsteden HC, et al. Expression of platelet-derived growth factor (PDGF) and PDGF receptors in human malignant mesothelioma in vitro and in vivo. J Pathol 1996;178:151–60.
14. Ceresoli GL, Zucali PA. Anti-angiogenic therapies for malignant pleural mesothelioma. Expert Opin Investig Drugs 2012;21:833–44.
15. Yap TA, Aerts JG, Popat S, Fennell DA. Novel insights into mesothelioma biology and implications for therapy. Nat Rev Cancer 2017;17:475–88.
16. Hilberg F, Roth GJ, Krssak M, Kautschitsch S, Sommergruber W, Tontsch-Grunt U, et al. BIBF 1120: triple angiokinase inhibitor with sustained receptor blockade and good antitumor efficacy. Cancer Res 2008;68:4774–82.
17. Tai WT, Shiau CW, Li YS, Chang CW, Huang JW, Hsueh TT, et al. Nintedanib (BIBF-1120) inhibits hepatocellular carcinoma growth independent of angiokinase activity. J Hepatol 2014;61:89–97.
18. Kutluk Cenik B, Ostapoff KT, Gerber DE, Brekken RA. BIBF 1120 (nintedanib), a triple angiokinase inhibitor, induces hypoxia but not EMT and blocks progression of preclinical models of lung and pancreatic cancer. Mol Cancer Ther 2013;12:992–1001.
19. du Bois A, Kristensen G, Ray-Coquard I, Reuss A, Pignata S, Colombo N, et al. Standard first-line chemotherapy with or without nintedanib for

advanced ovarian cancer (AGO-OVAR 12): a randomised, double-blind, placebo-controlled phase 3 trial. Lancet Oncol 2016;17:78–89.
20. Eisen T, Loembe AB, Shparyk Y, MacLeod N, Jones RJ, Mazurkiewicz M, et al. A randomised, phase II study of nintedanib or sunitinib in previously untreated patients with advanced renal cell cancer: 3-year results. Br J Cancer 2015;113:1140–7.
21. Reck M, Kaiser R, Mellemgaard A, Douillard JY, Orlov S, Krzakowski M, et al. Docetaxel plus nintedanib versus docetaxel plus placebo in patients with previously treated non-small-cell lung cancer (LUME-Lung 1): a phase 3, double-blind, randomised controlled trial. Lancet Oncol 2014;15: 143–55.
22. Richeldi L, du Bois RM, Raghu G, Azuma A, Brown KK, Costabel U, et al. Efficacy and safety of nintedanib in idiopathic pulmonary fibrosis. N Engl J Med 2014;370:2071–82.
23. Grosso F, Steele N, Novello S, Nowak AK, Popat S, Greillier L, et al. Nintedanib plus pemetrexed/cisplatin in patients with malignant pleural mesothelioma: phase II results from the randomized, placebo-controlled LUME-meso trial. J Clin Oncol 2017;35:3591–600.
24. Scagliotti GV, Gaafar R, Nowak AK, Reck M, Tsao AS, van Meerbeeck J, et al. LUME-meso: design and rationale of the phase III part of a placebo-controlled study of nintedanib and pemetrexed/cisplatin followed by maintenance nintedanib in patients with unresectable malignant pleural mesothelioma. Clin Lung Cancer 2017;18:589–93.
25. Kilkenny C, Altman DG. Improving bioscience research reporting: ARRIVE-ing at a solution. Lab Anim 2010;44:377–8.
26. Torok S, Rezeli M, Kelemen O, Vegvari A, Watanabe K, Sugihara Y, et al. Limited tumor tissue drug penetration contributes to primary resistance against angiogenesis inhibitors. Theranostics 2017;7:400–12.
27. Yang F, Tang X, Riquelme E, Behrens C, Nilsson MB, Giri U, et al. Increased VEGFR-2 gene copy is associated with chemoresistance and shorter survival in patients with non-small-cell lung carcinoma who receive adjuvant chemotherapy. Cancer Res 2011;71:5512–21.
28. Meng F, Speyer CL, Zhang B, Zhao Y, Chen W, Gorski DH, et al. PDGFRalpha and beta play critical roles in mediating Foxq1-driven breast cancer stemness and chemoresistance. Cancer Res 2015;75:584–93.
29. Turner N, Grose R. Fibroblast growth factor signalling: from development to cancer. Nat Rev Cancer 2010;10:116–29.
30. Li Q, Yano S, Ogino H, Wang W, Uehara H, Nishioka Y, et al. The therapeutic efficacy of anti-vascular endothelial growth factor antibody, bevacizumab, and pemetrexed against orthotopically implanted human pleural mesothelioma cells in severe combined immunodeficient mice. Clin Cancer Res 2007;13:5918–25.
31. Marek LA, Hinz TK, von Massenhausen A, Olszewski KA, Kleczko EK, Boehm D, et al. Nonamplified FGFR1 is a growth driver in malignant pleural mesothelioma. Mol Cancer Res 2014;12:1460–9.
32. Lo Iacono M, Monica V, Righi L, Grosso F, Libener R, Vatrano S, et al. Targeted next-generation sequencing of cancer genes in advanced stage malignant pleural mesothelioma: a retrospective study. J Thorac Oncol 2015;10:492–9.
33. Hylebos M, Van Camp G, van Meerbeeck JP, Op de Beeck K. The genetic landscape of malignant pleural mesothelioma: results from massively parallel sequencing. J Thorac Oncol 2016;11:1615–26.
34. Bueno R, Stawiski EW, Goldstein LD, Durinck S, De Rienzo A, Modrusan Z, et al. Comprehensive genomic analysis of malignant pleural mesothelioma identifies recurrent mutations, gene fusions and splicing alterations. Nat Genet 2016;48:407–16.
35. Awasthi N, Hinz S, Brekken RA, Schwarz MA, Schwarz RE. Nintedanib, a triple angiokinase inhibitor, enhances cytotoxic therapy response in pancreatic cancer. Cancer Lett 2015;358:59–66.
36. Garay T, Juhasz E, Molnar E, Eisenbauer M, Czirok A, Dekan B, et al. Cell migration or cytokinesis and proliferation?–revisiting the "go or grow" hypothesis in cancer cells in vitro. Exp Cell Res 2013;319:3094–103.
37. Klominek J, Baskin B, Hauzenberger D. Platelet-derived growth factor (PDGF) BB acts as a chemoattractant for human malignant mesothelioma cells via PDGF receptor beta-integrin alpha3beta1 interaction. Clin Exp Metastasis 1998;16:529–39.
38. Okada A, Yaguchi T, Kanno T, Gotoh A, Nakano T, Nishizaki T. PDGF-D/PDGF-betabeta receptor-regulated chemotaxis of malignant mesothelioma cells. Cell Physiol Biochem 2012;29:241–50.
39. Wollin L, Wex E, Pautsch A, Schnapp G, Hostettler KE, Stowasser S, et al. Mode of action of nintedanib in the treatment of idiopathic pulmonary fibrosis. Eur Respir J 2015;45:1434–45.
40. Andre F, Cortes J. Rationale for targeting fibroblast growth factor receptor signaling in breast cancer. Breast Cancer Res Treat 2015;150:1–8.
41. Abu-Hijleh MF, Habbal OA, Moqattash ST. The role of the diaphragm in lymphatic absorption from the peritoneal cavity. J Anat 1995;186:453–67.
42. Shinohara H. Lymphatic system of the mouse diaphragm: morphology and function of the lymphatic sieve. Anat Rec 1997;249:6–15.
43. Kindler HL, Ismaila N, Armato SG 3rd, Bueno R, Hesdorffer M, Jahan T, et al. Treatment of malignant pleural mesothelioma: American society of clinical oncology clinical practice guideline. J Clin Oncol 2018: JCO2017766394.
44. Jayson GC, Kerbel R, Ellis LM, Harris AL. Antiangiogenic therapy in oncology: current status and future directions. Lancet 2016;388: 518–29.
45. Goel S, Wong AH, Jain RK. Vascular normalization as a therapeutic strategy for malignant and nonmalignant disease. Cold Spring Harb Perspect Med 2012;2:a006486.
46. Van der Veldt AA, Lubberink M, Bahce I, Walraven M, de Boer MP, Greuter HN, et al. Rapid decrease in delivery of chemotherapy to tumors after anti-VEGF therapy: implications for scheduling of anti-angiogenic drugs. Cancer Cell 2012;21:82–91.
47. Ackermann M, Hilberg F, Konerding MA. Abstract B09: Nintedanib inhibits tumor and vessel growth and leads to vascular normalization in A549-NSCLC-xenografts. Mol Cancer Ther 2015;14:B09–B.
48. Ackermann M, Kim YO, Wagner WL, Schuppan D, Valenzuela CD, Mentzer SJ, et al. Effects of nintedanib on the microvascular architecture in a lung fibrosis model. Angiogenesis 2017;20:359–72.